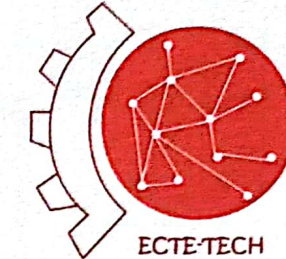


People's Democratic Republic of Algeria
University of Larbi Ben M'hidi - Oum El Bouaghi -
Institute of Technology - Aïn M'lila -



ATTENDANCE CERTIFICATE

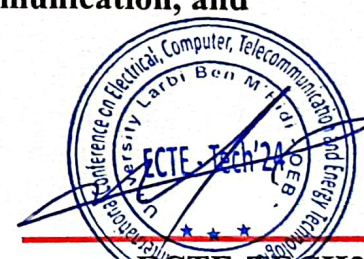


This certificate is proudly presented to:
Amina TAMER

For attending ECTE-TECH24 and presenting the paper entitled:
Effects of Power Supply Phase Imbalance on the Electrical and Mechanical Performance of Induction Motor

The first International Conference on Electrical, Computer, Telecommunication, and Energy Technologies (ECTE-TECH24)

Authors: **TAMER amina, Bilal Djamel Eddine Cherif**



ECTE-TECH24
General Chairwoman
Dr. Nassima MELLAL



Effects of Power Supply Phase Imbalance on the Electrical and Mechanical Performance of Induction Motor

Amina Tamer

Second cycle department , Higher School of Electrical and Energy Engineering of Oran. Algeria
Laboratory L2GEGI, University Ibn Khaldoun Tiaret, Algeria
tamer.amina@esgee-oran.dz

Bilal Djamel Eddine Cherif

Electrical Engineering Laboratory (LGE), Department of Electrical Engineering, Faculty of Technology, University of M'sila, University Pole, Road Bourdj Bou Arreiridj, M'sila
cherif.bilaldjamaleddine@univ-msila.dz

Abstract— This paper provides a comprehensive analysis of the electrical and mechanical behavior of induction motors under unbalanced fault conditions. We propose a novel detection method that utilizes the Hilbert-Huang spectral envelope of the stator current to identify and localize the unbalance faults. The results demonstrate the efficacy of this fault detection and localization approach, highlighting its ability to effectively address the various operational degradations of induction motors caused by this related fault.

Keywords— *Induction motor, fault, supply phase imbalance, supply phase interruption, envelope spectral.*

I. INTRODUCTION

The electric machine is a crucial component in electric drives and electromechanical energy conversion. Given its pivotal role in production chains, it can also become a potential weak link. This is why monitoring of electrical machines has advanced significantly in the industrial sector. Enhancing the operational safety and extending the service life of these drives have become increasingly crucial. Among these, the cage asynchronous motor is particularly favored due to its robustness and cost-effectiveness [1].

In recent decades, significant research has focused on the early detection and diagnosis of faults in induction motors. Various techniques are employed for this purpose, including vibration analysis, acoustic analysis, and thermographic analysis. However, these methods are primarily recommended for identifying mechanical faults, such as bearing issues and imbalance [2].

In recent years, a new technique has gained traction, which leverages the analysis of stator current. This approach is noteworthy because both stator current provide comprehensive information about nearly all potential faults in asynchronous motors. The analysis of stator currents in the frequency domain is still the most widely used method, particularly for stationary conditions. This approach is highly effective because the frequency domain spectrum reveals critical information about most electrical and mechanical faults that can occur in an electrical machine [3].

Numerous studies have demonstrated that analyzing the stator current of asynchronous machines effectively reveals the majority of electrical and mechanical faults in electric drives. This approach to monitoring electric drives has been extensively covered in publications over the past decade. However, it's potential to identify a broader range of faults that could impact not just the motor but the entire transmission system remains underexplored [4].

The primary advantage of this technique is its ability to detect a wide range of electromechanical faults using only the stator current. This eliminates the need for additional sensors dedicated to measuring mechanical quantities or vibrations. Another advantage is that current sensors are already integrated into all electric drive control systems, allowing for measurement without interrupting machine operation [5].

This paper addresses the diagnosis and localization of faults related to power supply imbalances in squirrel-cage induction motors. It introduces the use of the Hilbert-Huang spectral envelope of stator current to identify and pinpoint issues caused by the unbalanced power ..

II. VOLTAGE SUPPLY FAULT

We will analyze the electrical and mechanical behavior of asynchronous motors when subjected to imbalances and power phase cuts, focusing on scenarios involving voltage supply faults during stationary operating periods[6].

A. Single-phase voltage fault

The voltages of the actual three-phase machine are described by the following equation [7]:

$$\begin{cases} K * V_a(t) = V_m \sin(2\pi ft) \\ V_b(t) = V_m \sin(2\pi ft - 2\pi/3) \\ V_c(t) = V_m \sin(2\pi ft - 4\pi/3) \end{cases} \quad (1)$$

For a single-phase fault, K is a real factor within the interval [0, 1].

B. Two-phase voltage fault

The voltages of the three-phase machine are represented by the following equation [7]:

$$\begin{cases} K * V_a(t) = V_m \sin(2\pi ft) \\ K * V_b(t) = V_m \sin(2\pi ft - 2\pi/3) \\ V_c(t) = V_m \sin(2\pi ft - 4\pi/3) \end{cases} \quad (2)$$

For a two-phase fault, K is a real factor within the interval $[0, 1]$.

C. Three-phase voltage fault

The voltages of the three-phase machine can be described by the following equation:

$$\begin{cases} K * V_a(t) = V_m \sin(2\pi ft) \\ K * V_b(t) = V_m \sin(2\pi ft - 2\pi/3) \\ K * V_c(t) = V_m \sin(2\pi ft - 4\pi/3) \end{cases} \quad (3)$$

For a three-phase fault, K is a real factor within the interval $[0, 1]$.

III. DETECTION TECHNIQUES EMPLOYING STATOR CURRENT SPECTRUM AND ENVELOPE SPECTRUM ANALYSIS

In this section, we will explore two signal processing techniques.

A. Fast Fourier Transform algorithm (FFT)

Fig. 1 illustrates the fast Fourier transform algorithm.

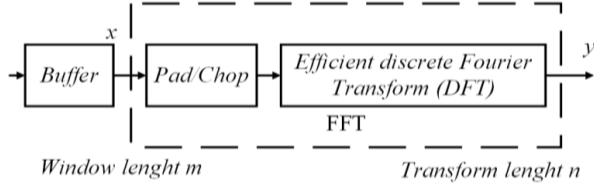


Fig. 1.: Algorithm of FFT.

To implement the Fast Fourier Transform (FFT) for vectors of length N using MATLAB, follow the instructions provided in the equations below [8]:

$$y = fft(x) \quad (4)$$

Where:

$$x(k) = \sum_{j=1}^N x(j) \omega_N^{(j-1)(k-1)} \quad (5)$$

$$x(j) = \left(\frac{1}{N} \right) \sum_{k=1}^N x(k) \omega_N^{-(j-1)(k-1)} \quad (6)$$

$$\omega_N = e^{(-2\pi i)/N} \quad (7)$$

B. Envelope analysis (ENV)

The Hilbert transform of a signal $x(t)$ is defined by the following equation:

$$H[x(t)] = \frac{1}{\pi} \int_{-\infty}^{+\infty} \frac{x(t)}{t - \tau} d\tau = \hat{x}(t) \quad (8)$$

\hat{x}

Where: $\hat{x}(t)$ represents the imaginary component of the analytic signal and $z(t)$ which is defined as follows[9] [10]:

$$z(t) = x(t) + j \hat{x}(t) = x(t) + jH[x(t)] = A(t)e^{j\varphi(t)} \quad (9)$$

Where: $H[x(t)]$ is the Hilbert transform of $x(t)$.

$$\varphi(t) = \arctg \left[\frac{\hat{x}(t)}{x(t)} \right] \quad (10)$$

In practice, the envelope method involves several processing steps of the raw time signal before obtaining the final result. These steps are summarized below[11]:

- **Step 1:** Filtering the raw signal to remove unwanted components;
- **Step 2:** We use the Hilbert transform to compute the envelope;
- **Step 3:** The envelope spectrum is calculated, from which fault information can be extracted.

IV. SIMULATION RESULTS AND DISCUSSION

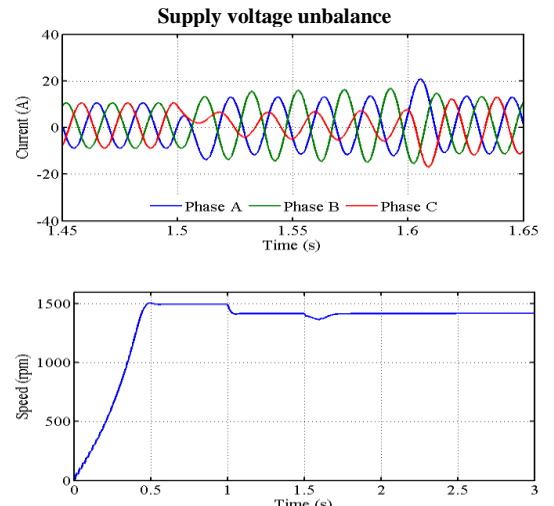
The parameters of the induction motor used in the simulation are presented in Table I .

Table I.

TABLE I. PARAMETERS OF INDUCTION MOTOR

Supply voltage	380V
Coupling	Δ
Nominal power	3kW
Nominal current	7A
Nominal speed	1410 rpm
Stator resistance	6 Ω
Rotor resistance	2.8 Ω
Stator cyclic inductance	0.5668 Ω
Rotor cyclic inductance	0.5142 Ω
Mutual inductance	0.5142 Ω
Number of pole pairs	2
Moment of inertia	0.058 K_{gm}^2
Viscous friction coefficient	0.005 Nm.s.rad

Fig. 2, presents the simulation results for supply voltage unbalance ($K=0.5$) illustrating the disturbances caused by single-phase voltage faults.



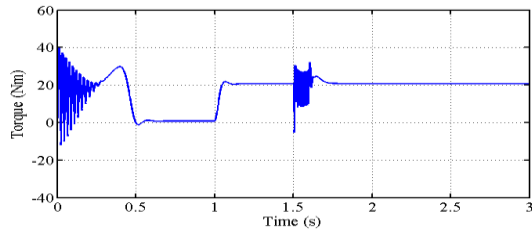


Fig. 2: Stator current, speed and torque in the case of supply voltage unbalance

Fig. 3, presents the simulation results for supply voltage unbalance ($K=0.5$) illustrating the disturbances caused by two-phase voltage faults.

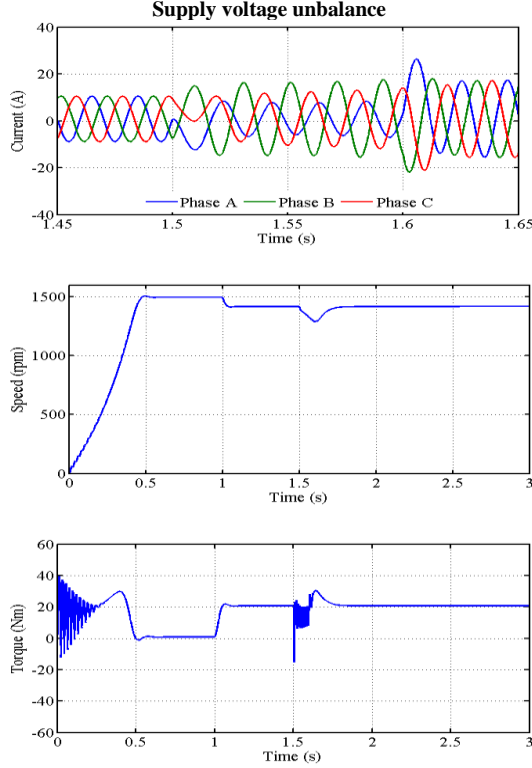


Fig. 3: Stator current, speed and torque in the case of supply voltage unbalance

Fig. 4, presents the simulation results for supply voltage unbalance ($K=0.5$) illustrating the disturbances caused by three-phase voltage faults.

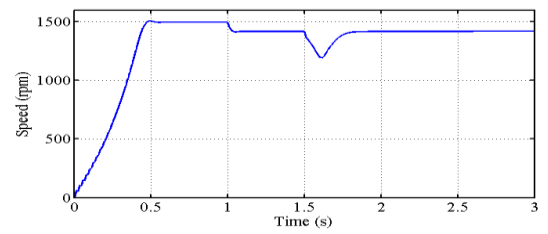
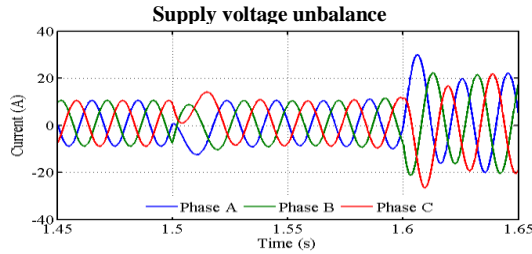


Fig. 4: Stator current, speed and torque in the case of supply voltage unbalance

The simulation results are shown in Figures 2, 3 and 4, which provide a comprehensive representation of the motor's behavior under both normal and abnormal operating conditions. These figures detail stator currents, speed and electromagnetic torque, providing insight into the motor's dynamic response during fault scenarios. In our case, the fault is introduced when the motor reaches a steady state at $t = 1.5$ s and removed at $t = 1.6$ s. Under normal conditions, the motor operates in a steady state characterized by stable electrical and mechanical quantities. The stator currents have a periodic sinusoidal waveform, the speed stabilizes at its nominal value, and the electromagnetic torque oscillates minimally around its mean value, ensuring smooth operation. In addition, faults such as unbalance have a pronounced effect on the mechanical performance of the motor, causing a reduction in speed and fluctuations in the electromagnetic torque, with the specific effects varying according to the type of fault. Analyzing the fault conditions reveals distinct changes in the stator current behavior for each fault scenario compared to normal operation, serving as clear indicators of the presence of the fault.

Fig. 5, depicts the FFT spectrum and ENV for the unbalanced.

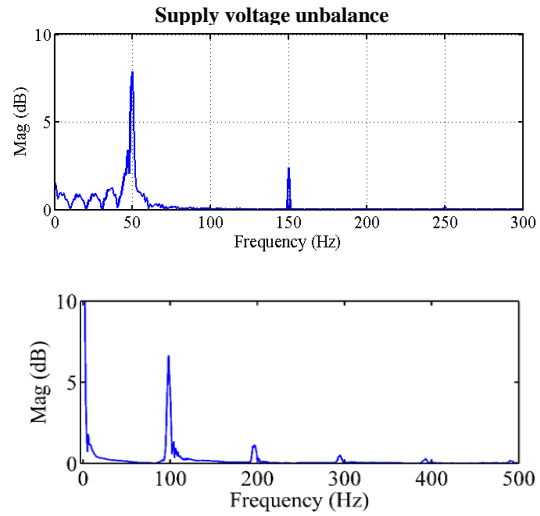


Fig. 5: FFT and ENV of the stator current

The key characteristics of Hilbert Huang's spectral envelope method are outlined as follows:

- Elimination of the fundamental frequency (50 Hz) from the current spectrum;
- Shift all frequency signatures left by 50 Hz;
- The removal of the fundamental frequency enhances the visibility of typically weak defect frequency signatures;
- The enhanced visibility of defect frequency signatures enables the use of a linear scale instead of a semi-logarithmic scale;
- By eliminating the fundamental frequency, a distinct frequency component characteristic of the fault is revealed, rather than the three multiple sidebands. This is exemplified by the signature of an imbalance phase fault.

The spectral analysis and spectral envelope of the stator current during a phase imbalance fault are illustrated in Fig. 5. The FFT spectrum reveals the presence of f_s (50 Hz) and $3f_s$ (150 Hz). In the Hilbert-Huang spectral envelope, the fundamental harmonic f_s (50 Hz) is not visible due to the envelope effect, which enhances the visibility of other components and shifts all frequencies by 50 Hz. This shift explains the presence of the harmonic ($f_s + 2f_s = 150$ Hz) at the frequency of $2f_s$ (100 Hz).

V. CONCLUSION

This paper deals with the diagnosis and detection of imbalance phase faults in a three-phase, two-level inverter-fed induction motor controlled by the *SVM* strategy.

Firstly, the effect of imbalance phase faults on the inverter-induction motor system. Simulation results show that the current waveforms of the motor indicate it is not feasible to maintain long-term service continuity in the presence of an imbalance phase fault.

The paper also introduces a diagnostic technique based on FFT and ENV for detecting imbalance phase faults in inverters. This diagnostic technique provides a powerful tool for identifying phase imbalance faults in inverter-driven motors. By focusing on the distinct harmonic signatures

introduced by faults and leveraging the complementary strengths of FFT and ENV, the method improves both fault detection sensitivity and diagnostic accuracy, making it a robust solution for modern industrial systems.

VI. References

- [1] I. Choudira, D. Khodja, S. Chakroune “ Continuous Wavelet Technique for Detection of Broken Bar Faults in Induction Machine” Traitement du Signal, Vol36, n:02,pp: 171-176.2019.
- [2] S. Tianyu, C. Chaoobo, W. Shenghang, et al. “Inverter open circuit fault diagnosis based on residual performance evaluation”. IET Power Electronics, vol. 16, no 15, pp. 2560-2576, 2023.
- [3] Z. Gang et YU, Jingrong. “Open-circuit fault diagnosis for cascaded H-bridge multilevel inverter based on LS-PWM technique”. CPSS Transactions on Power Electronics and Applications, 2021, vol. 6, no 3, pp. 201-208, 2021.
- [4] R. Saeed, T. Hadi, K. Naser Vosoughi, et al. “An overview of lifetime management of power electronic converters”. Ieee Access, 2022, vol. 10, pp. 109688-109711, 2022.
- [5] C. Bilal Djamel Eddine, B. Azeddine, et T, Mostefa. “An automatic diagnosis of an inverter IGBT open-circuit fault based on HHT-ANN”. Electric Power Components and Systems, 2020, vol. 48, no 6-7, pp. 589-602, 2020.
- [6] F. JiSheng et Y. Wei. “Review of parametric fault prediction methods for power electronic circuits”. Engineering Research Express, vol. 3, no 4, pp. 042002, 2021.
- [7] C. Chaobo, Y. Ying, Z. Binbin, et al. “The Diagnostic Method for Open-Circuit Faults in Inverters Based on Extended State Observer”. Mathematical Problems in Engineering, vol. 2021, no 1, pp. 5526173, 2021.
- [8] L. Jin et Z. Youmin. “A diagnosis method of inverter open-circuit fault based on interval sliding mode observer ”. In : 2022 4th International Conference on Smart Power & Internet Energy Systems (SPIES). IEEE, pp. 604-608, 2022.
- [9] H. Byong Jo, H. Dae Yeon, J. Pooreum, et al. “Offline Fault Diagnosis for 2-Level Inverter: Short-Circuit and Open-Circuit Detection”. Electronics, vol. 13, no 9, pp. 1672, 2024.
- [10] C. Antonio J. Marques et B. Fernando. “Diagnostics and Fault Tolerance in DC-DC Converters and Related Industrial Electronics Technologies”. Electronics, vol. 12, no 10, pp. 2341, 2023.
- [11] F. Masoud, V. Bhanu Teja, S. Rahman, et al. “ AC power cycling test setup and condition monitoring tools for SiC-based traction inverters”. IEEE Transactions on Vehicular Technology, vol. 72, no 10, pp. 12728-12743, 2023.